Journal of Tissue Viability 26 (2017) 172–179

Contents lists available at ScienceDirect

Journal of Tissue Viability

journal homepage: www.elsevier.com/locate/jtv

Off loading wheelchair cushion provides best case reduction in tissue deformation as indicated by MRI

Evan Call, MS, CSM [a, *], Thomas Hetzel, PT, ATP [b], Chad McLean [a], Joshua N. Burton [c], Craig Oberg, PhD [a]

[a] Weber State University, Ogden, UT, USA
[b] Aspen Seating/Ride Designs, USA
[c] University of Utah, SLC, UT, USA

ARTICLE INFO

Article history:
Received 29 December 2015
Received in revised form
15 May 2017
Accepted 16 May 2017

Keywords:
MRI
Tissue deformation
Off loading cushion
Air cell cushion

ABSTRACT

Off-loading or the Orthotic approach to wheelchair seating has been used successfully to provide seating that optimizes tissue protection at the ischial tuberosities (ITs), sacrum and greater trochanters. Recent publications indicate the significance of preventing tissue compression to reduce ulcer formation. Comparative Magnetic Resonance Imaging (MRI) of individuals seated on two cushion types provides direct evidence of tissue unloading resulting in the reduction in tissue compression. Measurement of tissue compression in MRI images provides the cumulative impact of compression and shear resulting in ultimate tissue thickness documented here. In this study's application of MRI to off-loading cushions (OLC), an alternate form of tissue protection was observed. Instead of incorporating immersion and envelopment, loads were transferred from high-risk areas, such as bony prominences, to lower risk soft tissues. This method shows both shearing and compression of load bearing tissues in seated individuals with the OLC in place. Tissue thickness measurements determined by MRI analysis indicate that the OLC provides greater reduction in tissue deformation than the air cell cushion (ACC). Deformation of tissues loaded by the OLC is not significantly different from the deformations seen with the ACC. This research represents the first reported use of MRI to document the comparative off-loading capabilities of two cushions and the resultant tissue compression and ulceration risk. While MRI analysis may not be incorporated in daily cushion prescription, this paper proposes a methodology in which MRI analysis of tissue deformation on comparative cushions allows the determination of best-case cushion selection for reduction of ischial pressure ulcer (PU) risk.

1. Introduction

In seating prescription, the question of best fit for an individual's needs is often addressed using pressure mapping with the goal to identify high-pressure regions that predict high-risk areas for future tissue failure and possible pressure injury. While pressure mapping accuracy and stability of calibration has been shown to fall short of ideal [1], it is used with some success to assist in the process of selecting the best options available in wheelchair cushion prescription [2].

Recent research indicates that forces exerted while sitting deform the load bearing tissue [3] Tissue deformation is the most likely cause of tissue damage over the bony prominences of wheelchair users [4,5] Magnetic Resonance Imaging (MRI) is the best available method to measure tissue deformation of persons seated on wheelchair cushions due to its ability to image the target tissue in multiple dimensions. The use of MRI to obtain tissue force deflection data for use in Finite Element Analysis (FEA) has been demonstrated by Levy et al. [6] and others [7,8]. In addition, the use of MRI to measure tissue deformation and anatomical features was reported by Sonenblum et al. [9], with their results defining best-case method and analysis of anatomical features. The research by Sonenblum et al. was published after the conclusion of our study, but supports the findings we obtained.

Recent attention has focused on the use of MRI to examine the forces responsible for tissue deformation in wheelchair seating [6].

* Corresponding author.
E-mail addresses: evan@ec-service.net (E. Call), tom@aspenseating.com (T. Hetzel), chad_Mclean@homedepot.com (C. McLean), joshua.burton@utah.edu (J.N. Burton), coberg@weber.edu (C. Oberg).

http://dx.doi.org/10.1016/j.jtv.2017.05.002
0965-206X/

While MRI will not replace pressure mapping in wheelchair seating prescription, recent use of MRI and FEA has demonstrated the positive benefits of pressure redistribution cushions, specifically the air cell cushion (ACC), due to their reduction of stresses responsible for tissue deformation and damage [6]. With this information kept in mind, a research approach was taken to determine the relative performance of an off-loading cushion (OLC) in comparison to the industry standard ACC for multiple individuals at significant risk for tissue damage.

The use of pressure mapping alone is unable to completely predict tissue deformation-based risk [10]. Our use of MRI supplements enhances the pressure maps, allowing us to measure an individual's tissue deformation under loaded and unloaded conditions. These data provide the necessary reference points to observe tissue deformation and calculate the tissue stresses observed in sitting on the tested surfaces.

1.1. Cushion principles of performance

ACCs minimize high pressure points by evenly redistributing pressure across the entire seating surface. ACCs operate by maximizing immersion and envelopment, and are optimized by adjusting air between the body and the drop or sling seat. This is done until the distance between the cushion support surface is approximately 1.25 cm – 2 cm (½" to ¾"), thus optimizing contact with the body (envelopment).

An OLC protects high-risk tissues over boney prominences by displacing the damaging forces to surrounding lower-risk soft tissues. For example, off-loading of the ischial tuberosities (ITs), sacrum, and the trochanters is accomplished by loading the mid-gluteus maximus, the gluteus medius, and proximal hamstrings [8,11] (Fig. 1). This balance between support and off-loading further enables the OLC to improve and optimize pelvic alignment and functional postures [12].

Historically, concerns raised with OLCs were primarily based on the early use of rings or donuts following vaginal birthing to relieve injured and swollen tissues from the load of sitting. R.A. Crewe reported damage to soft tissue in a study of 17 ring cushions available in the industry in 1987. [2,13] Shear injury occurred when tissue in contact with the ring allowed adjacent soft tissues to sag into the center of the ring. While it was not clear that the study demonstrated a high risk to the tissue associated with the use of ring cushions, it was concluded that ring and doughnut type supports contributed to soft tissue injury. Therefore, these devices have not been recommended for pressure ulcer prevention since 1992 [6,14] and a general prohibition has remained in effect in the healthcare world against the use of donut-like OLCs [15,16]. It is of value to note that Crewe's results were mixed; some suggested benefit from using ring cushions and some showed tissue damage [13]. The author's experience has also suggested that the problem is not as critical as Crewe originally indicated. The industry has followed Crewe's suggestions while the mixed results from Crewe's research were unclear regarding the benefits or possible harm connected to OLCs. The authors believe these mixed results are due to the area of contact and the angle of the contact surface, which was not measured in Crewe's study. In this study, the angle of contact was measurable in the MRI images and stayed consistent throughout.

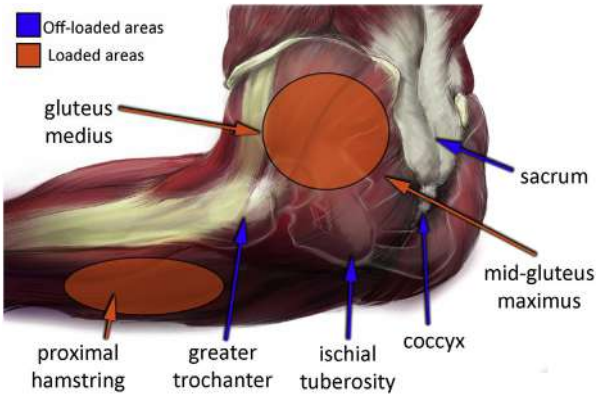

Fig. 1. View of loaded areas surrounding the ITs and resulting off-loaded areas using OLC.

Fifteen years of successful clinical reports using custom OLCs pushed the authors to research the reasons behind the success with these products [11]. Differences in function between OLCs and ACCs, that justify further research, include: tissue protection at the bony prominences, improved stability, and provision for airflow to improve microclimate. With the principles of OLCs being applied to off-the-shelf cushions, this raised a question: can an off-the-shelf OLC provide tissue protection and low tissue deformation over bony prominences, thus protecting the tissue? This study initiates the evaluation of these differences, along with the overall performance of OLCs using MRI to compare/contrast tissue deformation of OLCs vs. enveloping cushions.

The purpose of this study was to measure the tissue deformation of wheelchair users' tissue over the ITs and at the trochanters while seated on either the ACC industry standard envelopment cushion, or on an OLC. The metric of interest was tissue thickness at the ITs and at the trochanter, which was measured by collecting MRI images in the unloaded and loaded state on each of the two test cushions with the data used to compare OLC and ACC.

2. Methodology

2.1. Subjects

An Institutional Review Board (IRB) approval number 14-002 was granted by the Weber State University Institutional Review Board. All precautions for research involving human subjects were utilized throughout the data collection process, including collecting informed consent from all participants. All collected data was maintained per HIPAA privacy laws.

Demographics of the volunteers are listed in Table 1. MRI images were collected from 11 active volunteers, 10 with spinal cord injury (SCI) and 1 able bodied (control). Out of the 10 volunteers with SCI, 4 were female, 7 were male; the mean time since injury was 18.17 years, and the mean body weight was 65.4 kg. The American Spinal Injury Association impairment score is listed, as is the individual's relative level of atrophy [17] (Table 1).

The relative level of atrophy was determined by the physical therapist working on the study by completing the International Standards for Neurological Classification of Spinal Cord Injury (ISNCSCI) impairment scale [18]. The level of atrophy was determined for each volunteer in relation to the nature of the SCI and completeness of the injury. It should be noted that the pool of volunteers was weighted toward active individuals and professional athletes. Considering atrophy below the level of injury is independent of activity level or professional activities; the authors determined this was an ideal volunteer pool based on their ability to transfer and tolerate assisted transfers.

2.2. Experimental procedure

MRI images were produced using a Fonar Stand up MRI (Model

Table 1
Volunteer demographics.

Vol	Gender	Age	Weight	Diagnosis	ASIA Scale[a]	Years Post Injury	Activity Level	Relative Level of Atrophy
	M/F	Yrs	kg	SCI/Level of Injury			Professional athlete, Athletic, Active, Inactive	0-5 (0 = none to 5 = most severe)
1	F	44	52.7	T12	A	22	Pro athlete	4
2	M	53	65.9	T12	C	31.833	Pro athlete	3
3	M	27	75.0	able	E	n/a	athletic	0
4	M	45	72.7	T5	A	13.75	active	3
5	F	31	56.8	T11	B	13.5	pro athlete	3
6	F	30	45.5	T11	A	2.83	pro athlete	2
7	M	42	65.9	T5/6	A	16.83	pro athlete	4
8	M	29	65.5	T5/6	A	10.5	active	5
9	M	43	70.5	T3/4	A	29.75	active	3
10	M	56	93.2	C6/7	C	27	active	2
11	F	45	55.9	T4	A	13.75	pro athlete	5

[a] American Spinal Injury Association (ASIA) Impairment Scale.

0606010-00, Melville, New York) setup with a modified seat option for volunteers with paraplegia from SCI. A bead foam block seat with a cut-out for the MRI Thoracic Coil was positioned immediately beneath the volunteer. The order in which the volunteers sat on cushions was randomized for the test. Volunteers were returned to their personal sitting surface for approximately 5 min prior to each test (see MRI seat construction in Fig. 2A). Each volunteer wore loose fitting clothing (scrubs or sweats) and was scanned in three different sitting configurations:

1. Suspended in a sitting position with nothing contacting the skin.
2. Seated on a therapist configured inflated ACC.
3. Seated on a therapist configured OLC.

2.3. Configuration 1, suspended

The seating system of the MRI was modified by removing the back cushion, replacing it with adhesive strips of a hook and loop fastening system. A specially designed fabric trunk support was attached to the hook and loop fasteners. An integral abdominal panel was wrapped around the volunteer (Fig. 2B and C) and a thigh support was placed on the thoracic coil, so the volunteer's pelvis, when seated in the trunk support, would be allowed to free float with a minimum of 25–40 mm clearance over the coil when the thighs rested comfortably on the support.

Volunteers were transferred into the MRI using a safe 2-person transfer technique. A therapist palpated the tissue of the buttock to ensure that it was not resting on the thoracic coil and that the pelvis was in neutral alignment; level, not rotated. Blocks of 1.27 cm (½")

Fig. 2. Patient suspended in the Standup MRI during imaging (A). Support/suspension system used to suspend volunteers during data collection (A and B). Back plate with hook and loop straps used to suspend patient in air, during unloaded and loaded testing, to provide positioning and support (B and C). Molded bead seat with embedded thoracic imaging coil to facilitate image collection of the ITs and surrounding tissue (C).

and 2.54 cm (1″) thick bead foam were stacked on the MRI system's non-adjustable foot support, as needed, to ensure that the volunteer's feet were supported in the correct seating position. The hook and loop strapping and polyvinyl chloride (PVC) supports were used for stability and comfort (Fig. 2B).

2.4. Configurations 2 and 3, ACCs and OLCs

Thigh support was removed and the ACC or OLC was positioned on the seat, and the process repeated. Care was taken to ensure neutral pelvic alignment during scanning to provide repeatable images.

2.5. Scan protocol

An initial scan was performed to locate the inferior prominence of the ITs. Once the target area was located, a series of coronal (frontal) plane images were acquired in 6 mm slices through the body segment, capturing the ITs and the greater trochanters. MRI images were gathered using T1-weighted spin echo in 5 mm slices with a 1 mm gap between slices, for a total of 6 mm intervals and a 380 mm field of view. The echo time was minimized for the scanner at this field of view at 20 ms, and a repetition time (TR) of 150–600 ms, optimized automatically by the scanner for minimizing scan time. Images were labeled and saved for analysis. The MRI resolution is 0.5 mm, limiting measurement accuracy to the nearest 0.05 cm.

2.6. Image processing and analysis

Images were saved as DICOM files and processed with E-Film Light software by Merge Software Chicago IL, which includes measurement and annotation tools. Individual tissue and total tissue thickness inferior to each ITs was identified. Horizontal, vertical, and perpendicular tissue thickness were measured from the inferior prominence of the head of the femur (Fig. 3). Measurement function of the software was validated against anatomical landmarks to estimate accuracy and error.

2.7. Pressure mapping

Pressure maps were generated in a separate process immediately following MRI image collection by transferring the volunteer to a wheelchair with the same seat to back relationship as utilized in the MRI collection. Pressure maps were generated using the XSensor X2 pressure map (Calgary, CA), calibrated, and verified immediately prior to use. Map was consistently positioned in the well of the OLC using sensing area-cushion alignment and was placed by the physical therapist. Cushion inflation used in the MRI image collection was maintained through pressure mapping. The potential for mapping artifacts was minimized by following the control of pressure mapping confounding influences described in previous work [19]. The area of interest for the force values was the area directly below the ITs.

2.8. Stress and strain calculations

Stress was calculated using force readings from the pressure mapping data. Stress is equal to the applied force divided by the area; in this case, the area under the ITs. ITs locations were identified and the area under was an estimate based on the XSensor X2 pressure map cell size of 1 cm^2 (0.0001 m^2). Area was measured in m^2 to report stress in kilopascals (kPa). Strain was calculated by dividing the compressed tissue thickness from the ACCs by the non-compressed thickness. Values were determined from measurements of the MRI scans.

Statistical significance was determined using an Analysis of Variance (ANOVA) test with an alpha value of 0.05.

3. Results

3.1. Magnetic resonance imaging (MRI)

The tissues identified as inferior to the ITs are reported in Table 2. On average, fat was the thickest layer observed. The skin was frequently thin enough that it was difficult to measure using the available MRI software. Muscle tissue was not observed in four of the volunteers, presumably not present due to atrophy. Miscellaneous tissues were also observed, occasionally including

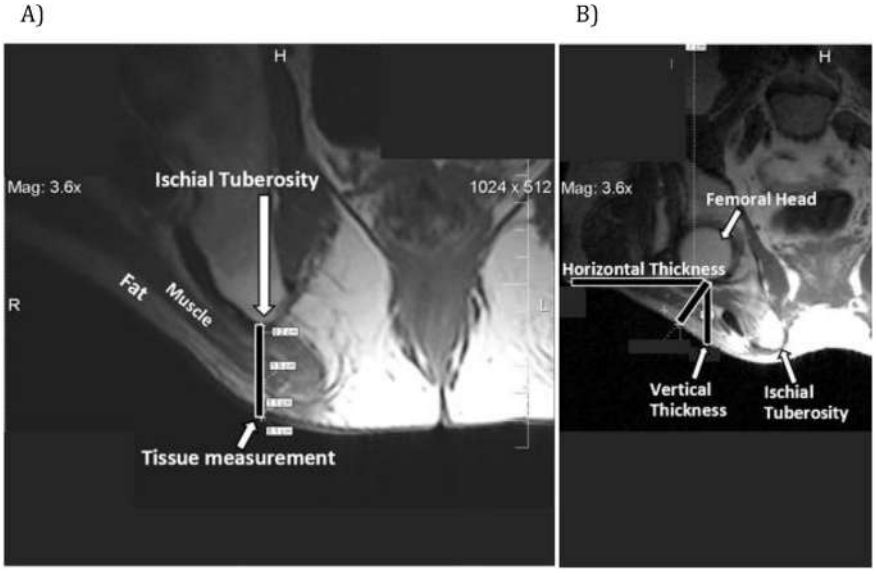

Fig. 3. (A) Examples of measurements to clarify the location of tissue thickness and tissue type under each ITs. (B) Examples of measurements made to determine whether off-loading was achieved during testing. Examples of measurement of the horizontal, vertical, and perpendicular tissue thickness in relation to the femoral head.

Table 2
Tissue type and thickness under the ITs—fully suspended/unloaded, OLC, and ACC. All measurements are in centimeters (cm).

Volunteer/Cushion Type		Muscle	Fat	Skin	Misc. Tissues[b]	Total Thickness
1	unloaded	0.00	2.20	0.00	0.45	2.65
	OLC	0.00	1.25	0.00	0.40	1.65
	ACC	0.00	0.70	0.00	0.10	0.80
2	unloaded	0.00	2.50	0.10	0.20	2.80
	OLC	0.00	1.65	0.00	0.20	1.85
	ACC	0.00	0.85	0.00	0.25	1.10
4	unloaded	0.70	2.45	0.00	0.25	3.40
	OLC	0.15	1.65	0.00	0.00	1.80
	ACC	0.35	0.65	0.00	0.00	1.00
5	unloaded	0.00	2.75	0.00	0.45	3.20
	OLC	0.00	1.30	0.00	0.50	1.80
	ACC	0.00	0.75	0.00	0.00	0.75
6	unloaded	0.15	2.75	0.00	0.00	2.90
	OLC	0.20	1.55	0.00	0.00	1.75
	ACC	0.20	0.60	0.00	0.00	0.80
7	unloaded	0.45	2.50	0.10	0.40	3.45
	OLC	0.35	2.10	0.10	0.00	2.55
	ACC	0.60	0.30	0.15	0.00	1.05
8	unloaded	0.60	0.75	0.00	0.00	1.35
	OLC	0.50	0.55	0.00	0.00	1.05
	ACC	0.40	0.40	0.00	0.00	0.80
9	unloaded	0.10	3.60	0.00	0.20	3.90
	OLC	0.10	2.85	0.00	0.20	3.15
	ACC	0.20	1.20	0.00	0.20	1.60
10	unloaded	2.40	1.20	0.05	0.05	3.70
	OLC	2.35	0.65	0.10	0.10	3.20
	ACC	0.55	0.60	0.15	0.05	1.35
11	unloaded	0.00	1.65	0.15	0.35	2.15
	OLC	0.00	0.80	0.05	0.40	1.25
	ACC	0.00	0.65	0.05	0.25	0.95
3[a]	unloaded	0.90	1.30	0.00	0.90	3.10
	OLC	2.50	0.00	0.00	0.90	3.30
	ACC	0.30	0.30	0.00	0.70	1.30

[a] Note: Volunteer 3 was the non-SCI control and was not wheelchair bound.
[b] Includes ischial bursas, intro-muscular fat, and undefined tissues.

interstitial fluid and/or ischial bursa. Soft tissue thickness under the ITs is reported in Fig. 4.

Tissue compression was determined by comparing the fully suspended tissue thickness for each volunteer to the tissue thickness measured using each of the two test cushions. The results demonstrate that the cushion type suggests a significant impact in the tissue compression in the area measured, and that compression of the fatty tissue represents much of that impact (Fig. 5).

Given that off-loading at-risk tissue moves the applied forces to adjacent tissue, it was necessary to examine the compression of tissue surrounding the head of the femur in 3 planes; horizontal, vertical, and perpendicular to the surface of the skin. This was done to investigate if relief of the ITs transferred greater risk to the soft tissues around the head of the femur (Fig. 6).

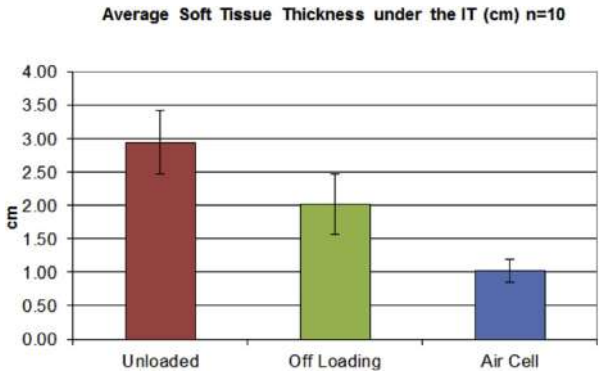

Fig. 4. Average soft tissue thickness under the ITs—unloaded, with OLCs, and ACCs. Error bars represent the 95th percentile confidence interval.

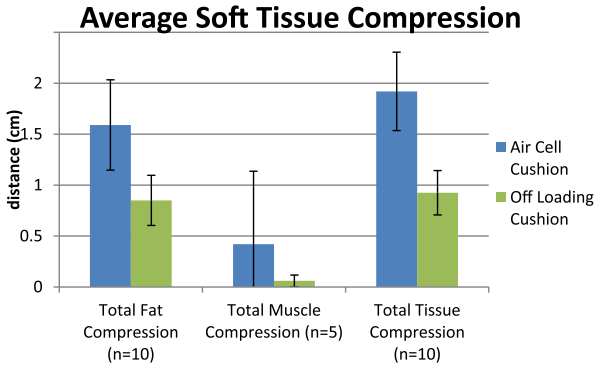

Fig. 5. Average total soft tissue compression is calculated by subtracting the distance from the edge to the ITs in a loaded state (either ACC or OLC) from the unloaded state. N = 5 for muscle compression, because no muscle was detected in 5 of 10 volunteers. Error bars represent the 95% confidence interval.

3.2. Pressure mapping and stress/strain

Pressure mapping of the individuals yielded force beneath the ITs and was used for calculating the stress on the soft tissue. For the ACC, the mean force/area is tightly clustered at the top of the range, representing a best seating case for air cell based pressure redistribution cushions. General use foam based cushions can be expected to exceed these values. Pressure mapping of the OLC yielded zero normal force on the soft tissue below the ITs. These data were

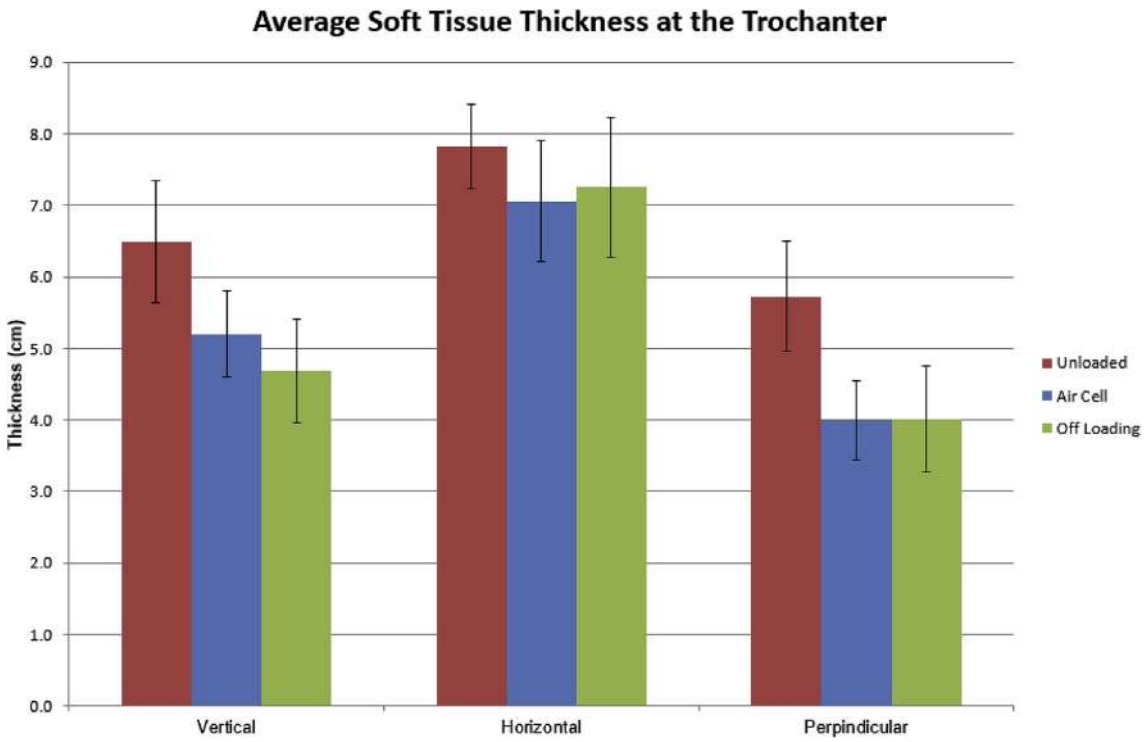

Fig. 6. Average soft tissue thickness around the trochanters, measured at the femoral head. Measured to show that the OLC did not increase risk of pressure injury around the femoral head as compared to the ACC. Error bars represent the 95% confidence interval.

processed to provide estimated tissue stress and strain (Table 3).

The average force under the ITs was measured at 16.28 N for the ACC and was assumed to be 0 N in the off-loaded state of the OLC. The average strain under the ITs was 0.64 for the ACC and 0.30 for the OLC. Statistical analysis (paired T-test) of the difference yielded a p-value < 0.001. Average values exclude the non-SCI subject. Strain was calculated directly under the ITs only, and not for adjacent tissues due to methodology constraints.

4. Discussion

Use of MRI analysis has the potential to determine individual best case cushion selection for reduction of pressure ulcer risk. While pressure mapping provides an indication of pressure based risk, MRI analysis can provide measurement of tissue deformation in critical areas. The MRI results indicate that the soft tissue thickness under the ITs decreases when using the ACC compared to the OLC (Fig. 4). This finding implies higher tissue strain, thus the potential for greater tissue risk when sitting on the ACC vs. the OLC. This data suggests a re-evaluation of the previous assumption that the ACC is best case for reducing pressure injury risk [13].

One unanticipated outcome was that 40% of the persons studied showed no muscle under the ITs, which is consistent with the findings of Sonenblum et al. [13]. This was not related to sitting on an OLC or ACC, but merely a statement of the volunteers' anatomical condition. The lack of muscle decreases the overall soft tissue thickness, increasing the risk of tissue damage over bony prominences. This finding supports an argument for enhancing off-loading to areas with thicker muscle mass, resulting in increased tissue thickness and lower risk of pressure injury over the bony

Table 3
Mean force under the ITs, tissue stress, and strain directly beneath the ITs for each of the cushions tested.

Volunteer	ACC					OLC	
	Mean Area under ITs (m^2)	Mean Force (N)	Stress (kPa)	Tissue Compression (cm)	Strain	Tissue Compression (CM)	Strain
1	0.00090	7.51	8.35	1.85	0.70	1.00	0.38
2	0.00060	7.74	12.90	1.70	0.61	0.95	0.34
3	N/A	N/A	N/A	1.80	0.58	−0.20	−0.06[a]
4	0.00100	20.74	20.74	2.40	0.71	1.60	0.47
5	0.00090	11.66	12.96	2.45	0.77	1.40	0.44
6	0.00100	17.72	17.72	2.10	0.72	1.15	0.40
7	0.00090	9.93	11.03	2.40	0.70	0.90	0.26
8	0.00090	18.04	20.05	0.55	0.41	0.30	0.22
9	0.00090	17.94	19.94	2.30	0.59	0.75	0.19
10	0.00070	14.30	20.43	2.35	0.64	0.50	0.14
11	0.00060	11.04	18.40	1.20	0.56	0.90	0.42
Average[b]	0.008	13.66	16.25	1.93	0.64	0.95	0.33

N/A – Not Available.
[a] Negative strain indicates that the tissue was elongated instead of compressed.
[b] Excluding data from Subject 3 (control).

prominences.

Several studies address the risk to muscle or skin due to deformation or hypoxia [20,21], but little information is available on fat. This deficiency may be due to fat's highly deformable nature. The data in this study suggest that fat deformation may be responsible for the greater portion of total tissue compression in loaded settings. Knowing that tissue compression is implicated as risk of ulceration, the high deformations seen in the fat suggests looking further at fat as a potential initiator of superficial injury rather than deep tissue injury. OLC's transition the loading to the gluteus (maximus, medias, and minimus), underlying piriformis, and the quad muscle areas to protect the ischium, potentially decreasing the risk of pressure injury. These areas of muscle mass would A fat-specific MRI study, analyzing and modeling fat deformation during cushion use, would allow for better estimates of tissue stress and strain and better determination of fatty tissues injury risk.

The ischial bursa appeared to be visible in two of the volunteers; however, the ischial bursa is a structure that is generally difficult to observe in MRI images, and its presence or absence could be an indicator of tissue changes related to time post SCI injury. Furthermore, without the collection of indicators of inflammation we have no indication of the impact of the bursa and its thickness on tissue risk.

The strain analysis was incomplete and used to identify particular trends in strain, rather than actual events. Tissue deformation occurred on both the ACC and the OLC, as shown in Table 3. Decreases in tissue thickness on the OLCs are not due to direct compression, but a result of tension in the tissues. E.G. When a person sits, the tissue stretches, resulting in fat deformation. Volunteer 3 (the control) showed slightly increased tissue thickness while sitting on the OLC, which is believed to be due to the tissues sagging into the central cavity of the OLC.

Overall, the strain is trending to be significantly less on the OLC than the ACC ($p < 0.001$), and never goes above the suggested 50% threshold for tissue injury [22]. There cannot be a comparison of stress values at the ITs, as none were taken for the OLC, due to the fact that the introduction of a pressure map onto the cushion would have distorted tissue displacement and rendered the data inaccurate. The conjecture is that as the ITs is suspended in air by the OLC, the normal force on the ITs is zero.

5. Conclusions

MRI analysis showed that the use of an OLC significantly decreased the amount of tissue compression inferior to the IT's when compared to an ACC ($p < 0.001$, paired *t*-test). Since the OLC redistributes loading force from the IT's to other tissues, it is important to know that the other bony prominences are not placed at greater risk due to transferred load. Our analysis shows that there was no greater loading at the trochanter when using an OLC. This suggests that while the OLC is providing greater protection at the ITs, it does not increase the distortion risk to the tissue at the trochanter, as compared to the ACC.

Forty percent of the wheelchair users tested had no identifiable muscle tissue inferior to the ITs. In those that did have both muscle and fatty tissue, there was greater compression in the fatty tissues than in the muscle, suggesting that the compression affected fat more than muscle. This indicates the need to explore whether or not these individuals are at greater risk for pressure injury.

In our study transfer of loading to soft tissues at the gluteus and the resulting deformation was not examined, however volumetric analysis of MRI images can be used to determine the resulting deformation of loaded soft tissues [23]. Unfortunately, previous work using volumetric analysis of MRI images does not report a comparison between ACC and OLC. In our two-dimensional analysis of tissues at the trochanter we did not see load transfer based deformation.

Previous work by Gefen [22] and others [24] has suggested that approximately 50% strain in tissue would be the threshold for pressure injury. Considering that there are a large number of factors that would influence the tissue's susceptibility to damage, the best possible protection for the tissue is to provide the greatest margin of safety by providing a seating environment that reduces tissue deformation and strain as much as possible.

The MRI images gathered for this study were acquired under lowest cost constraints, but the process provided a best possible location and a best possible image at location under these conditions. Higher resolution imaging would increase accuracy and allow for a more complete analysis of tissue strains, providing a better estimate of pressure injury risk and mitigation.

Use of MRI in measuring tissue deformation in seated individuals is important when trying to understanding a cushion's impact on tissue deformation. This makes MRI data valuable to both designers and prescribers; however, it is understood that cost makes MRI not feasible in prescription. The method described in this paper is meant to illuminate the promise for better understanding the effect of wheelchair cushions on the tissues of the pelvic region.

References

[1] Sprigle S, Dunlop W, Press L. Reliability of bench tests of interface pressure. Assistive Technol Off J RESNA 2003;15(1):49–57.
[2] Brienza D, Karg P, Geyer M, Kelsey S, Trefler E. The relationship between pressure ulcer incidence and buttock-seat cushion interface pressure in at-risk elderly wheelchair users. Arch Phys Med Rehab 2001;82(4):529–33.
[3] Shabshin N, Zoizner G, Herman A, Ougortsin V, Gefen A. Use of weight-bearing MRI for evaluating wheelchair cushions based on internal soft-tissue deformations under ischial tuberosities. J Rehab Res Dev 2010;47(1):31–42.
[4] Bouten CV, Breuls RG, Peeters EA, Oomens CW, Baaijens FP. In vitro models to study compressive strain-induced muscle cell damage. Bio Rheol 2003;40(1–3):383–8.
[5] Gawlita D, Li W, Oomens C, Baaijens FP, Bader D, Bouten C. The relative contributions of compression and hypoxia to development of muscle tissue damage: an in vitro study. Ann Biomed Eng 2007;3(2):273–84.
[6] Levy A, Kopplin K, Gefen A. An Air-cell-based cushion for pressure ulcer protection remarkably reduces tissue stresses in the seated buttocks with respect to foams: finite element studies. J Tissue Viab. 2014;23:13–23.
[7] Linder-Ganz E, Gefen A. Stress analyses coupled with damage laws to determine biomechanical risk factors for deep tissue injury during sitting. J Biomech Eng 2009;131. 011003–1 -13.
[8] Sopher R, Nixon C, Gorecki C, Gefen A. Effects of intramuscular fat infiltration, scarring and spasticity on the risk for sitting-acquired deep tissue injury in spinal cord injury patients. J Biomech Eng 2011;133(2). 021011-1 -12.
[9] Soneblum S, Sprigle S, McKay J, Winder R. 3D anatomy and deformation of the seated buttocks. J Tissue Viab 2015;24:51–61.
[10] Gefen A, Levine J. The false premise in measuring body-support interface pressures for preventing serious pressure ulcers. J Med Eng Technol 2007;31(5):375–80.
[11] Corbet B. 21st century seating. New Mobility. Available from: http://www.newmobility.com/2004/07/21st-century-seating/; [Accessed 29 May 2014].
[12] Collins F. Sitting: pressure ulcer development. Nurs Stand 2001;15(22):54–8.
[13] Crewe RA. Problems of rubber ring nursing cushions and a clinical survey of alternative cushions for ill patients. CARE-Sci Pract June 1987:9–11.
[14] Grey J, Enoch S, Harding K. ABC of wound healing. BMJ 25 Feb 2006;332:472–5.
[15] Haesler E, editor. Prevention and treatment of pressure ulcers: clinical practice guideline. National pressure ulcer advisory panel. European pressure ulcer advisory panel and pan Pacific pressure injury alliance. Cambridge media: Perth, Australia; 2014.
[16] AHCPR Publication No 92-0047. Panel for the prediction and prevention of pressure ulcers in adults; clinical practice guideline, number 3. Rockville, MD: Agency for Health Care Policy and Research, Public Health Service, US Department of Health and Human Services; May 1992.
[17] Maynard FM, Bracken M, Creasey G, Ditunno J, Donovan W, Ducker T, et al. International standards for neurological and functional classification of spinal cord injury. Spinal Cord 1997;35:266–74.
[18] American Spinal Injury Association. International standards for neurological classification of spinal cord injury. http://www.asia-spinalinjury.org/elearning/ASIA_ISCOS_high.pdf.

[19] Call E, Baker L. How does bed frame design influence tissue interface pressure? A comparison of four different technologies designed for long-term or home care. J Tissue Viab 2007;17:22–9.
[20] Gawlitta D, Oomens C, Bader D, Baaijens F, Bouten C. Temporal differences in the influence of ischemic factors and deformation on the metabolism of engineered skeletal muscle. J Appl Physiol 2007;103:464–73.
[21] Ceelen K, Gawlita D, Bader D, Oomens C. Numerical analysis of ischemia – and compression-induced injury in tissue-engineered skeletal muscle constructs. Ann Biomed Eng 2010;38(3):570–82.
[22] Gefen A, van Nierop B, Bader D, Oomens C. Strain-time cell-death threshold for skeletal muscle in a tissue-engineered model system for deep tissue injury. J Biomech 2008;41(9):2003–12.
[23] Brienza D, Vallely J, Karg P, Akins J, Gefen A. An MRI investigation of the effects of user anatomy and wheelchair cushion type on tissue deformation. J tissue Viab 2017. http://dx.doi.org/10.1016/j.jtv.2017.04.001.
[24] Breuls RGM, Bouten CVC, Oomens CWJ, Bader DL, Baaijens FPT. Compression induced cell damage in engineered muscle tissue: An *In Vitro* model to study pressure ulcer aetiology. Ann Biomed Eng 2003;31:1357–64.